

# Further Investigations of the ClO Rotational Spectrum

Brian J. Drouin, Charles E. Miller,\* Edward A. Cohen, Georg Wagner,† and Manfred Birk‡

*Jet Propulsion Laboratory, California Institute of Technology, Pasadena, California 91109-8099; \*Department of Chemistry, Haverford College, Haverford, Pennsylvania 19041-1392; and †Institut für Methodik der Fernerkundung Deutsches Zentrum für Luft- und Raumfahrt e.V., Münchner Str. 20, D-82234 Wessling, Germany*

E-mail: [cmiller@haverford.edu](mailto:cmiller@haverford.edu)

Received October 23, 2000; in revised form March 2, 2001

Pure rotational transitions of the chlorine monoxide radical have been observed up to  $v = 2$  in the  $X_1^2\Pi_{3/2}$  and  $X_2^2\Pi_{1/2}$  states and transitions of the  $^{35}\text{Cl}^{18}\text{O}$  isotopomer have been observed in natural abundance. Additionally, rotational transitions for levels up to  $J' = 115/2$  have been measured in the far infrared. These data have been merged with the existing microwave, submillimeter, and high-resolution infrared transition frequencies and fit simultaneously with a set of isotopically independent parameters. Isotopic substitution of both the Cl and O atoms has enabled the first determination of the electron spin–rotation constant  $\gamma = -296.0(43)$  MHz as well as the Born–Oppenheimer corrections to the rotational constants. © 2001 Academic Press

## INTRODUCTION

The importance of the halogen monoxides in atmospheric ozone depletion chemistry has motivated their spectroscopic characterization (1). High-resolution spectroscopy provides a method for remote sensing of these gases at the sub-parts-per-billion level. Pure rotational transitions of the chlorine monoxide radical, ClO, have proven especially valuable in remote sensing applications, enabling NASA's Microwave Limb Sounder to retrieve accurate global stratospheric ClO concentrations on a daily basis (2).

Rotational spectra of ClO  $X_1^2\Pi_{3/2}$  and  $X_2^2\Pi_{1/2}$  in the  $v = 0$ , 1 states have been investigated previously in this laboratory (3–5) and elsewhere (6–8). These studies employed an effective Hamiltonian to obtain rotational, fine and hyperfine constants. Coxon (9) provided direct measurements of the  $X^2\Pi$  fine structure interval  $A_v$  through analysis of the VUV absorption spectrum. High-resolution infrared spectra of ClO provided complementary information on the rotational energy levels for  $J \leq 87/2$  in  $v = 0, 1$  (10, 11) and partial characterization of  $v = 2$  (11, 12).

Experiments on the atmospherically important processes  $\text{Cl} + \text{O}_3$  (13, 14) and  $\text{OCIO} + h\nu$  (15–17) have shown that these reactions generate ClO in vibrational levels up to  $v = 5$  and  $v = 15$ , respectively. Recent experiments in this laboratory have resulted in the measurement of BrO (18) and IO (19) pure rotational spectra in excited vibrational levels of the  $X_1$  and  $X_2$  states containing up to  $8000\text{ cm}^{-1}$  of internal energy. We reinvestigated the rotational spectrum of ClO hoping to observe similar levels of vibrational excitation; however, the dc discharge source chemistry that had been successful for creating excited BrO and IO failed to produce vibrationally excited ClO.

Nevertheless, using traditional source chemistry, improvements in the spectrometer sensitivity enabled us to observe pure rotational transitions of ClO  $X_1$  and  $X_2$  in the  $v = 2$  level for the first time. Additionally,  $^{35}\text{Cl}^{18}\text{O}$  transitions were observed in natural abundance for  $v = 0$  levels of both  $X_1$  and  $X_2$  for three well-separated  $J + 1 \leftarrow J$  multiplets as well as transitions from one such group for  $^{37}\text{Cl}^{18}\text{O}$   $X_1$ ,  $v = 0$  and  $^{35}\text{Cl}^{18}\text{O}$   $X_1$ ,  $v = 1$ . These data have been fit simultaneously with with new high-resolution far infrared Fourier transform rotational data, as well as existing rotational transition frequencies and high-resolution infrared data using an isotopically independent Dunham parameter set. The resulting spectroscopic constants provide an improved description of the ClO  $X^2\Pi$  state and enable us to determine the electron spin–rotation constant  $\gamma$  and deviations of the rotational constant from the Born–Oppenheimer approximation.

## EXPERIMENTAL

The details of the submillimeter spectrometer used in this study have been described previously (20, 21). Measurements were made in selected regions between 70 and 850 GHz. Submillimeter sources not previously described include a backward wave oscillator operating between 520 and 705 GHz and an antiparallel planar Schottky pair multiplier (22). Spectra were recorded with the submillimeter beam passed twice through a 1-m-long, 7.3-cm-diameter, temperature-controlled glass absorption cell.

Recent experiments have shown that highly vibrationally excited BrO (18) and IO (19) are created efficiently in a dc discharge plasma of  $\text{O}_2/\text{X}_2$ . This source chemistry was investigated for ClO, but it resulted in only minor vibrational excitation

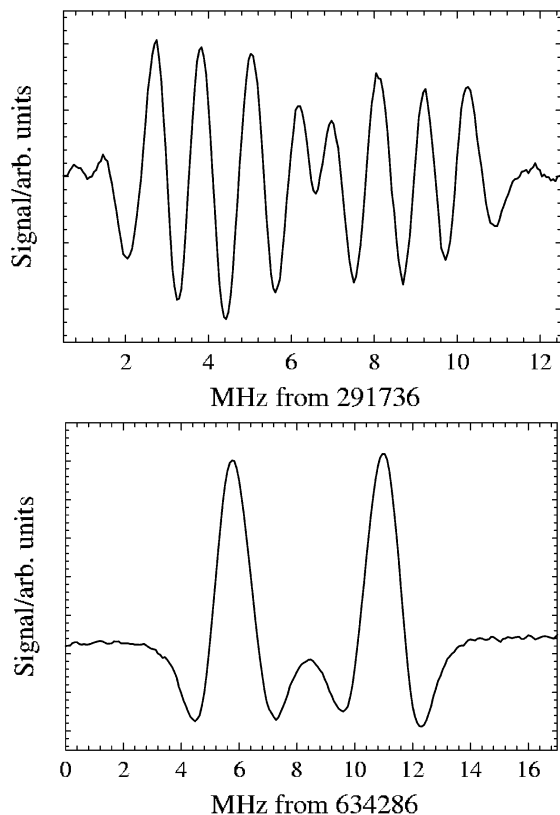


**FIG. 1.** Two scans of  $^{35}\text{Cl}^{18}\text{O } ^2\Pi_{3/2} v=0$  transitions in natural abundance showing a hyperfine quartet of  $\Lambda$ -doublets for  $J=17/2-15/2$  (top) and a  $\Lambda$ -doublet of unresolved hyperfine quartets for  $J=37/2-35/2$  (bottom).

and produced spectra with relatively poor signal-to-noise due to Stark broadening. We therefore reverted to the standard method of generating ClO by passing a mixture of  $\text{Cl}_2$  and  $\text{O}_2$  through an external microwave discharge. Optimal signals were obtained by combining the  $\text{Cl}_2$  and  $\text{O}_2$  gases prior to the microwave discharge cavity and adjusting the gas pressures while monitoring a strong spectral feature. Typical flow pressures, measured at the exit of the absorption cell with a capacitance manometer, were  $\sim 4$  mTorr  $\text{Cl}_2$  and  $\sim 60$  mTorr  $\text{O}_2$ .

Under these optimized conditions strong  $v=0$  transitions of both spin-orbit states exhibited signal-to-noise (S/N) ratios in excess of 1000. Corresponding transitions in the  $v=1, 2$  levels were observed with good S/N after averaging 8–16 scans. Similar signal strengths were observed for the weak  $\Delta F=0$  transitions of  $^{35,37}\text{ClO}$  in  $v=0$ . The spectrometer sensitivity was also sufficient to record strong  $^{35}\text{Cl}^{18}\text{O } v=0$  transitions in natural abundance with good S/N after averaging 32 scans. Examples of the  $^{35}\text{Cl}^{18}\text{O}$  spectra are given in Fig. 1.

The methods used to measure the ClO rotational spectrum in the far infrared have been described previously (23). The DLR experimental apparatus consisted of a temperature controlled multipass absorption cell connected to a Bruker IFS 120 HR high-resolution Fourier transform spectrometer and a

1.4 K silicon bolometer. Spectra were recorded at 296 K with  $0.00278 \text{ cm}^{-1}$  resolution and an optical path of 72 meters. Signal-to-noise in the  $15\text{--}75 \text{ cm}^{-1}$  range was improved by placing a  $100 \text{ cm}^{-1}$  low-pass filter immediately in front of the detector. ClO concentrations of ca.  $5 \times 10^{13} \text{ molecules cm}^{-3}$  were generated efficiently from the reaction of  $\text{Cl} + \text{Cl}_2\text{O}$ . The reaction mixture was flowed through the absorption cell to maintain a total pressure of 1500 Pa and a residence time of less than 3 seconds.

## DATA ANALYSIS

Spectral assignments were straightforward using line positions predicted from previous microwave (3, 4) and infrared (10–12) work. The submillimeter and far infrared transition frequencies measured in this study were combined with all previous high-resolution  $X^2\Pi$  data and analyzed simultaneously. All data were weighted inversely as the square of their uncertainties. The data include transitions from the  $^{35,37}\text{Cl}^{16,18}\text{O}$  isotopomers and span the quantum numbers  $3/2 \leq J' \leq 115/2$  and  $0 \leq v \leq 2$  for  $^{35}\text{Cl}^{16}\text{O}$ . The fit results are given in Tables 1–3. Uncertainties are based on the weighted least-squares fit to 324 millimeter and submillimeter, 161 far infrared, and 326 infrared frequencies (10–12) with a reduced rms of 0.93. In the tables and elsewhere in the text, the numbers in parentheses are  $1\sigma$  uncertainties in units of the least significant figure. The measured and predicted ClO rotational transition frequencies are available through the submillimeter and microwave spectral line catalog (24) on-line at <http://spec.jpl.nasa.gov>. An electronic file containing the final fitting parameters, transition frequencies and fitting residuals has been deposited with the Journal.

The data have been fit with a Hamiltonian incorporating isotopic relations through Dunham expansion of the parameters involving vibration, rotation, and electronic fine structure. The interpretation of these parameters for  $^2\Lambda$  ( $\Lambda > 0$ ) molecules is discussed by Brown and Watson (25) in their work describing methods for decorrelating the parameters  $\gamma$  and  $A_D$ ,

$$\begin{aligned} \mathcal{H}_v = & T_v + B_v \mathbf{N}^2 - D_v \mathbf{N}^4 + H \mathbf{N}^6 \\ & + (1/2)[(A_v + A_{D_v} \mathbf{N}^2 + A_H \mathbf{N}^4), L_z S_z]_+ \\ & + \gamma \mathbf{N} \cdot \mathbf{S} + (1/4)[(p_v + p_{D_v} \mathbf{N}^2), (\Lambda_+^2 S_- N_- \\ & + \Lambda_-^2 S_+ N_+)]_+ - (q/2)(\Lambda_+^2 N_-^2 + \Lambda_-^2 N_+^2), \quad [1a] \end{aligned}$$

where

$$\begin{aligned} B_v &= \sum_l Y_{l,1}(v+1/2)^l \\ D_v &= -\sum_l Y_{l,2}(v+1/2)^l \\ H &\approx Y_{03} \end{aligned} \quad [1b]$$

and

$$\begin{aligned} \mathcal{H}_{hfs} = & aI_zL_z + b_F\mathbf{I} \cdot \mathbf{S} + c(I_zS_z - \mathbf{I} \cdot \mathbf{S}/3) \\ & + (1/2)d(\Lambda_+^2I_-S_- + \Lambda_-^2I_+S_+) + C_I\mathbf{I} \cdot \mathbf{N} \\ & + [(eQq_1 + N_zS_z eQq_S)(3I_z^2 - \mathbf{I}^2) \\ & + eQq_2(I_x^2 - I_y^2)]/[4I(2I - 1)]. \end{aligned} \quad [1c]$$

The principal advantage of this Hamiltonian is that each parameter has a well-defined isotope dependence. This has allowed fitting the spectra of all three ClO isotopomers with a single set of isotopically invariant parameters. Not shown throughout Eq. [1] are the vibrational dependencies and centrifugal distortion terms analogous to those demonstrated for  $B_v$  and  $D_v$  in Eq. [1b]. We define isotope dependencies such that if an operator is multiplied by an expression of the form

$$Z_{l,n}(v + 1/2)^l [N(N + 1)]^n \quad [2a]$$

then

$$Z_{l,n} \propto r \mu^{-(l+2n)/2}, \quad [2b]$$

where  $r$  contains the mass and/or nuclear moment isotope dependence of  $Z_{00}$ . The Born–Oppenheimer corrections to the most precisely determined parameters are best described in terms of the mass-independent parameters  $U_{l,n}$  and  $\Delta_{l,n}^A$  (26) as shown in the equation

$$Y_{l,n} = \mu^{-(l+2n)/2} U_{l,n} \left( 1 + \frac{m_e \Delta_{l,n}^O}{M_O} + \frac{m_e \Delta_{l,n}^{Cl}}{M_{Cl}} \right). \quad [3]$$

Le Roy (27) has defined isotope dependent quantities,  $\delta_{l,n}^A$ , such that

$$Y_{l,n} = \mu^{-(l+2n)/2} U_{l,n} - \delta_{l,n}^O - \delta_{l,n}^{Cl}. \quad [4]$$

All of the isotopic relations were fixed within the parameter input file for the program SPFIT (28) and the independent parameters determined using global fits to all isotopic data. Because there are no infrared data for the  $^{18}\text{O}$  species, the full isotope dependence of  $Y_{10}$  could not be determined. Only  $Y_{10}$  and  $\delta_{10}^{Cl}$  values are reported. Parameters are defined relative to  $^{35}\text{Cl}^{16}\text{O}$  using fixed ratios of the reduced masses (29), quadrupole moments, and magnetic moments (30). Note that the terms referred to here as Born–Oppenheimer corrections contain all contributions of order  $\mu^{-2}$  for  $Y_{01}$  and  $\mu^{-5/2}$  for  $Y_{11}$ .

The rotation, vibration, and rovibrational coupling constants derived from the fit are presented in Table 1. The Born–Oppenheimer corrections are of the expected sign and order of magnitude. They are  $\{\Delta_{10}^{Cl}, \Delta_{01}^{Cl}, \Delta_{01}^O, \Delta_{11}^O\} = \{-0.794(53), -1.419(24), -2.240(15), -4.95(213)\}$ . It should be noted

**TABLE 1**  
 **$^{35}\text{ClO } X^2\Pi$  Mechanical Parameters**

Parameter	Value	Units	Isotope Dependence
$U_{01}/\mu$	18692.6545(123)	MHz	$\mu^{-1}$
$\delta_{01}^{Cl}$	0.4162(72)	MHz	$\mu^{-1}M_{Cl}^{-1}$
$\delta_{01}^O$	1.4385(94)	MHz	$\mu^{-1}M_O^{-1}$
$Y_{01}$	18690.79984(128)	MHz	
$U_{11}/\mu^{3/2}$	-177.9784(123)	MHz	$\mu^{-3/2}$
$\delta_{11}^O$	-0.0302(130)	MHz	$\mu^{-3/2}M_O^{-1}$
$Y_{11}$	177.94821(297)	MHz	
$Y_{21}$	-0.13740(99)	MHz	$\mu^{-2}$
$Y_{02}$	-39.87192(227)	kHz	$\mu^{-2}$
$Y_{12}$	38.4(55)	Hz	$\mu^{-5/2}$
$Y_{22}$	-14.44(253)	Hz	$\mu^{-3}$
$Y_{03}$	-0.015509(309)	Hz	$\mu^{-3}$
$Y_{10}$	853.642681(133)	cm $^{-1}$	
$\delta_{10}^{Cl}$	0.01063(71)	cm $^{-1}$	$\mu^{-1/2}M_{Cl}^{-1}$
$Y_{20}$	-5.518278(60)	cm $^{-1}$	$\mu^{-1}$
$Y_{30}$	-0.012560 <sup>a</sup>	cm $^{-1}$	$\mu^{-3/2}$

<sup>a</sup> Fixed parameter.

that the Born–Oppenheimer correction to  $Y_{11}$  is determined solely from the  $^{35}\text{Cl}^{18}\text{O } v=1, J=35/2 - 33/2$  doublet.  $Y_{22}$  and  $Y_{21}$  are both required to fit the  $v=2$  rotational data. The inclusion of  $Y_{22}$  improves the rms of the 10 measured frequencies for  $J' = 17/2, 21/2,$  and  $33/2$  from 117 to 57 kHz and their reduced rms from 1.95 to 0.80. The high- $J$  rotational transitions measured in the far infrared spectrum have enabled us to determine  $Y_{03}$  quite well, with the fitted value of -0.01551(31) Hz in very good agreement with the value of -0.01472 Hz calculated from  $Y_{10}, Y_{01},$  and  $Y_{11}$  via the Dunham relationships (31). Fits incorporating higher order parameters demonstrated that those parameters were poorly determined by the data and failed to produce a statistically significant improvement in the rms error. They were, therefore, excluded from the final fit.

The effective constants for  $^{35,37}\text{Cl}^{16}\text{O } v=0, 1$  determined in this study are not significantly different from those previously reported (4). In that study  $Y_{03}$  for  $^{35}\text{ClO}$  was fixed by Dunham relations to -0.015 Hz although it was not significantly determined by that data set. With the inclusion of the far infrared Fourier transform spectra, the value has been confirmed experimentally. In Table 1 the uncertainties of the parameters  $U_{01}$  and  $U_{11}$  are relatively large due to correlations with higher order parameters and the Born–Oppenheimer corrections. For comparison, the more precise values of  $Y_{01}$  and  $Y_{11}$  are listed in the table. The uncertainties in the ground state rotational constants,  $B_0$ , for both  $^{35}\text{ClO}$  and  $^{37}\text{ClO}$ , are approximately 0.4 kHz. The deviation of the  $Y_{10}$  values from a  $\mu^{-1/2}$  relationship is small but significant with respect to the experimental uncertainties.  $Y_{10}(^{35}\text{ClO})(\mu_{35}/\mu_{37})^{1/2}$  is 0.00030 cm $^{-1}$  smaller than the fitted value for  $^{37}\text{ClO}$ .  $Y_{30}$  is a fixed parameter calculated from the Dunham relations. Its inclusion in the fit produces some small changes in  $Y_{10}$  and  $Y_{20}$  from previously reported values.

The  $^{35}\text{ClO}$  values of the fine structure parameters are listed in Table 2. The fine structure interval,  $A_e = -321.9577 \text{ cm}^{-1}$ , was fixed to be consistent with the value determined by Coxon (9) for the vibrational ground state of  $^{35}\text{ClO}$  since it was impossible to determine from the present data. The vibrational dependence of the fine structure splitting was determined very well due to the simultaneous fitting of the  $^{35}\text{ClO}$  and  $^{37}\text{ClO}$  infrared data. The parameters  $A_{00}$ ,  $A_{20}$ , and  $A_{30}$  were determined from the vibrational level intervals calculated via the Dunham potential parameters for the  $X_1$  and  $X_2$  states (see below) and fixed during the fit. The inclusion of  $A_{20}$  in the fit alters  $A_{10}$  compared to the value reported by Burkholder *et al.* (11) but is necessary for the correct determination of  $Y_{20}$ . The change in  $A$  between  $v = 0$  and  $v = 1$  is, however, virtually identical to that in Ref. (11) since it is determined primarily by the data reported there.

The electron spin-rotation constant  $\gamma$  has been determined for the first time by fitting all the isotopic species simultaneously with fixed isotope relationships among the constants. The value  $\gamma = -296.0(43) \text{ MHz}$  is in reasonable agreement with  $-p/2 = -339.261(32) \text{ MHz}$ , suggesting that a single excited electronic state is responsible for most of the  $\Lambda$ -doubling in the  $X^2\Pi$  state. The sign and magnitude of  $p_{00}$  are consistent with a  $^2\Sigma^+$  perturbing state located approximately  $35,600 \text{ cm}^{-1}$  above  $X^2\Pi$  as pointed out in Refs. (6) and (9). The value of  $\gamma$  is highly correlated with that of  $A$ . Because of the constraints imposed by the isotope relations, the fitting routine maintains an almost constant value for the quantity  $(B - \gamma/2)^2/(A - 2B)$ . The calculated uncertainty in  $A_{01}$  is primarily due to the uncertainty in this quantity. These uncertainties largely cancel in the calculation of the spectrum. The previous analysis of the ground state spectrum of ClO done in this laboratory (4) contained the implicit assumption that  $\gamma = -p/2$ . As a result, the constants

TABLE 2  
 $^{35}\text{ClO } X^2\Pi$  Fine Structure Parameters

Parameter	Value	Units	Isotope Dependence
$A_e$	$-321.957710^a$	$\text{cm}^{-1}$	
$A_{00}$	$-.000114^a$	$\text{cm}^{-1}$	$\mu^{-1}$
$A_{10}$	$3.293426(39)$	$\text{cm}^{-1}$	$\mu^{-1/2}$
$A_{20}$	$-0.0075466^a$	$\text{cm}^{-1}$	$\mu^{-1}$
$A_{30}$	$0.0004715^a$	$\text{cm}^{-1}$	$\mu^{-3/2}$
$A_{01}$	$28.8805(162)$	MHz	$\mu^{-1}$
$A_{11}$	$0.1942(38)$	MHz	$\mu^{-3/2}$
$A_{21}$	$14.71(156)$	kHz	$\mu^{-2}$
$A_{02}$	$124.46(97)$	Hz	$\mu^{-2}$
$\gamma$	$-296.0(43)$	MHz	$\mu^{-1}$
$p_{00}$	$678.522(64)$	MHz	$\mu^{-1}$
$p_{10}$	$-4.716(153)$	MHz	$\mu^{-3/2}$
$p_{20}$	$-0.186(72)$	MHz	$\mu^{-2}$
$p_{01}$	$0.385(47)$	kHz	$\mu^{-2}$
$q$	$-0.9879(60)$	MHz	$\mu^{-2}$

<sup>a</sup> Fixed parameters.

TABLE 3  
 $^{35}\text{ClO } X^2\Pi$  Hyperfine Structure Parameters

Parameter	Value	Units	Isotope Dependence
$a_{00}$	$137.4799(252)$	MHz	$g_N$
$a_{10}$	$-2.5197(295)$	MHz	$g_N\mu^{-1/2}$
$b_F$	$15.65(35)$	MHz	$g_N$
$c_{00}$	$-95.19(53)$	MHz	$g_N$
$(b_F + 2c/3)_{00}$	$-47.805(52)^a$	MHz	$g_N$
$(b_F + 2c/3)_{10}$	$0.688(60)^b$	MHz	$g_N\mu^{-1/2}$
$d_{00}$	$174.705(35)$	MHz	$g_N$
$d_{10}$	$-3.338(41)$	MHz	$g_N\mu^{-1/2}$
$d_{01}$	$-0.65(33)$	kHz	$g_N\mu^{-1}$
$C_I$	$16.12(102)$	kHz	$g_N\mu^{-1}$
$eQq_{100}$	$-87.691(81)$	MHz	$Q$
$eQq_{110}$	$-0.636(93)$	MHz	$Q\mu^{-1/2}$
$eQq_{101}$	$-0.52(47)$	kHz	$Q\mu^{-1}$
$eQq_2$	$-117.71(221)$	MHz	$Q$
$eQq_S$	$0.313(71)$	MHz	$Q$

<sup>a</sup> Derived from  $b_F$  and  $c_{10}$ . The reduced uncertainty reflects their correlation.

<sup>b</sup> The parameters  $b_{F10}$  and  $c_{10}$  could not be decorrelated and were fit together.

which depend on the value of  $\gamma$  have not been significantly altered in the present work.

The Frosch-Foley (32) hyperfine parameters  $a$ ,  $b_F$ ,  $c$ , and  $d$ , as well as the nuclear spin-rotation constant  $C_I$ , for  $^{35}\text{ClO}$  are displayed in Table 3. The axial components of the quadrupole coupling tensor have been determined for the two spin-orbit states and are represented by the average value  $eQq_{100}$  and the difference between the  $X_2$  and  $X_1$  states given by  $eQq_S$ . The sign convention for the nonaxial term  $eQq_2$  is that of Endo *et al.* (33). A discussion of the sign conventions is included in a recent paper by Tamassia *et al.* (34). Centrifugal distortion on the larger hyperfine constants ( $d_{01}$  and  $eQq_{101}$ ) was included, as well as vibrational corrections linear in  $v$ . The quadrupole and magnetic moment ratios were fixed to  $r_Q = Q(^{35}\text{Cl})/Q(^{37}\text{Cl}) = 1.2688773$  and  $r_m = \mu_I(^{35}\text{Cl})/\mu_I(^{37}\text{Cl}) = 1.2013078$ , respectively (30). Parameters for the  $^{37}\text{Cl}$  and/or  $^{18}\text{O}$  isotopomers can be derived using the appropriate power of the ratio of reduced masses and/or nuclear moments. There are no changes in the main hyperfine constants from previously reported values which affect their interpretation in terms of molecular properties. The centrifugal distortion constants  $d_{01}$  and  $eQq_{101}$ , although not well determined, are both of the correct sign and magnitude and are consistent with similar constants recently reported for BrO (18). Previous ClO studies in this laboratory determined  $eQq_1$  separately for each spin-orbit state for the two main isotopes. In that work the uncertainties of the individual values of  $eQq_1$  were comparable to the difference between them. The present work shows that the difference,  $eQq_S$ , is more than four times larger than its uncertainty. Its value is consistent with that expected from the relativistic radial integrals calculated by Lindgren and Rosén (35) and the correction factors given by Pyykkö and Seth (36). The value here is slightly changed from the preliminary ClO value reported recently for comparison with

**TABLE 4**  
**ClO  $X^2\Pi$  Dunham Potential Parameters<sup>a</sup>**

Parameter	$^2\Pi_{3/2}$	$^2\Pi_{1/2}$	$^2\Pi_{\text{eff}}$
$r_e/\text{pm}$	156.89335	157.01460	156.95394
$a_0/\text{cm}^{-1}$	293226.5	291410.7	292317.8
$a_1$	-3.17276	-3.17342	-3.17309
$a_2$	6.45073	6.45454	6.45263
$a_3$	-11.67428	-11.63899	-11.65658
$a_4$	17.36530	17.07108	17.22507

$$^a V(\xi) = a_0(1 + a_1\xi + a_2\xi^2 + a_3\xi^3 + a_4\xi^4), \text{ where } \xi = (r - r_e)/r_e.$$

BrO (18), and the discussion in Ref. (18) is an adequate description of the origin of the term.

Table 4 presents the  $X^2\Pi$  Dunham potential energy coefficients (31) derived directly from the fitted parameters given in Table 1. Parameters describing the individual  $X_1^2\Pi_{3/2}$  and  $X_2^2\Pi_{1/2}$  potentials have also been determined from the relationships

$$Y_{l,n}^* = Y_{l,n} \pm A_{l,n}/2. \quad [5]$$

These potentials should be accurate for rovibrational energies up to  $2500 \text{ cm}^{-1}$ . We note that the Dunham potential parameters may be determined from a combination of rotational and vibrational parameters or from the rotational constants alone, inferring the harmonic vibrational frequency  $Y_{10}$  from the relationship

$$Y_{10} = 2 \left( \frac{Y_{01}^3}{-Y_{02}} \right)^{1/2}. \quad [6]$$

A comparison of the potential parameters calculated in each manner showed minimal differences between the two sets. Only the  $Y_{1,1}$  and  $Y_{1,2}$  constants were used to derive the  $a_i$  values in Table 4.

The displacement of the equilibrium positions has subtle ramifications for several of the Hamiltonian parameters. This is most relevant for  $\gamma$ , where the matrix element has a large contribution from an effective rotational constant *between* the  $X_1$  and  $X_2$  states. The fitted  $\gamma$  therefore absorbs contributions from all terms which have the same isotopic dependence as  $Y_{01}$ . One can extract a more accurate value of  $\gamma$ , denoted  $\gamma^*$ , by correcting  $\gamma$  for the vibrational overlap integral

$$S_{v,v} = \langle \Omega = 3/2, v || \Omega = 1/2, v \rangle. \quad [7]$$

The fitting parameter  $\gamma$  is related to  $\gamma^*$  via the equation

$$\gamma = S_{0,0}\gamma^* + 2B(1 - S_{0,0}), \quad [8]$$

where  $\gamma^*$  is the electron spin-rotation constant for the hypothetical  $S_{0,0} \equiv 1$  condition. The Dunham potentials yield  $S_{0,0} = 0.99989$ . The  $2B(1 - S_{0,0})$  term on the right hand side of Eq. [8] contributes 4.00 MHz to  $\gamma$ . This is the same order of

magnitude as the uncertainty in  $\gamma$  and, unlike the heavier halogen monoxides, does not significantly alter its interpretation.

## CONCLUSION

Measurements of the ClO  $X^2\Pi$  pure rotational spectrum have been extended to include transitions up to  $J' = 115/2$  and  $v = 2$ . Transitions from the  $^{35}\text{Cl}^{18}\text{O}$  isotopomer have also been observed. All ClO isotopic data have been fit simultaneously with a mass-independent Hamiltonian. This Hamiltonian, based on the Dunham expansion, allows independent determination of previously correlated parameters such as the electron-spin, rotation constant,  $\gamma$ , and the centrifugal distortion of the spin-orbit coupling constant,  $A_{01}$ . The fitted constants have been used to derive Dunham potentials for the effective  $X^2\Pi$  state as well as the individual  $X_1^2\Pi_{3/2}$  and  $X_2^2\Pi_{1/2}$  spin-orbit states. The refined spectroscopic constants presented here enable one to predict ClO rotational transition frequencies accurately up to 3 THz for all Cl and O isotopomers.

## ACKNOWLEDGMENTS

This paper presents research carried out at the Jet Propulsion Laboratory, California Institute of Technology, under contract with the National Aeronautics and Space Administration. The authors thank Tim Crawford for technical support.

## REFERENCES

1. R. P. Wayne, G. Poulet, P. Biggs, J. P. Burrows, R. A. Cox, P. J. Crutzen, G. D. Hayman, M. E. Jenkin, G. Lebras, G. K. Moortgat, U. Platt, and R. N. Schindler, *Atmos. Environ.* **29**, 2677–2881 (1995).
2. M. L. Santee, W. G. Read, J. W. Waters, L. Froidevaux, G. L. Manney, D. A. Flower, R. F. Jarnot, R. S. Harwood, and G. E. Peckham, *Science* **267**, 849–852 (1995).
3. R. K. Kakar, E. A. Cohen, and M. Geller, *J. Mol. Spectrosc.* **70**, 243–256 (1978).
4. E. A. Cohen, H. M. Pickett, and M. Geller, *J. Mol. Spectrosc.* **106**, 430–435 (1984).
5. J. J. Oh and E. A. Cohen, *J. Quant. Spectrosc. Radial. Transfer* **52**, 151–156 (1994).
6. T. Amano, E. Hirota, and Y. Morino, *J. Mol. Spectrosc.* **27**, 257–265 (1968).
7. T. Amano, S. Saito, E. Hirota, Y. Morino, D. R. Johnson, and F. X. Powell, *J. Mol. Spectrosc.* **30**, 275–289 (1969).
8. T. Amano and E. Hirota, *J. Mol. Spectrosc.* **66**, 185–187 (1977).
9. J. Coxon, *Can. J. Phys.* **57**, 1538–1552 (1979).
10. A. G. Maki, F. J. Lovas, and W. B. Olson, *J. Mol. Spectrosc.* **92**, 410–418 (1982).
11. J. B. Burkholder, P. D. Hammer, C. J. Howard, A. G. Maki, G. Thompson, and C. Chackerian, *J. Mol. Spectrosc.* **124**, 139–161 (1987).
12. R. S. Lowe and A. R. W. McKellar, *J. Mol. Spectrosc.* **79**, 424–431 (1980).
13. Y. Matsumi, S. Nomura, M. Kawasaki, and T. Imamura, *J. Phys. Chem.* **100**, 176–179 (1996).
14. S. Baumgartel, R. F. Delmdahl, K.-H. Gericke, and A. Tribukait, *Eur. Phys. J. D* **4**, 199–205 (1998).
15. H. F. Davis and Y. T. Lee, *J. Chem. Phys.* **105**, 8142–8163 (1996).
16. A. Furlan, H. A. Scheld, and J. R. Huber, *J. Chem. Phys.* **106**, 6538–6547 (1997).
17. M. Roth, C. Maul, and K. Gericke, *J. Chem. Phys.* **107**, 10,582–10,591 (1997).

18. B. J. Drouin, C. E. Miller, H. S. P. Muller, and E. A. Cohen, *J. Mol. Spectrosc.* **205**, 128–138 (2001).
19. C. E. Miller and E. A. Cohen, manuscript in preparation.
20. M. Birk, R. R. Friedl, E. A. Cohen, H. M. Pickett, and S. P. Sander, *J. Chem. Phys.* **91**, 6588–6597 (1989).
21. R. R. Friedl, M. Birk, J. J. Oh, and E. A. Cohen, *J. Mol. Spectrosc.* **170**, 383–396 (1995).
22. J. E. Oswald, T. Koch, I. Mehdi, A. Pease, R. J. Dengler, T. H. Lee, D. A. Humphrey, M. Kim, P. H. Siegel, M. A. Frerking, and N. R. Erickson, *IEEE Microwave Guided Wave Lett.* **8**, 232–234 (1998).
23. M. Birk and G. Wagner, *J. Geophys. Res. D*, **102**, 19,199–19,206 (1997).
24. H. M. Pickett, R. L. Poynter, E. A. Cohen, M. L. Delitsky, J. C. Pearson, and H. S. P. Muller, *J. Quant. Spectrosc. Radial. Transfer* **60**, 883–890 (1998).
25. J. M. Brown and J. K. G. Watson, *J. Mol. Spectrosc.* **65**, 65–74 (1977).
26. J. K. G. Watson, *J. Mol. Spectrosc.* **45**, 99–113 (1973).
27. R. J. Le Roy, *J. Mol. Spectrosc.* **194**, 189–196 (1999).
28. H. M. Pickett, *J. Mol. Spectrosc.* **148**, 371–377 (1991).
29. G. Audi and A. H. Wapstra, *Nucl. Phys. A*, **595**, 409–480 (1995).
30. J. H. Holloway, Ph.D Thesis, Massachusetts Institute of Technology, 1956.
31. J. L. Dunham, *Phys. Rev.* **41**, 721–731 (1931).
32. R. A. Frosch and H. M. Foley, *Phys. Rev.* **88**, 1337–1349 (1952).
33. Y. Endo, S. Saito, and E. Hirota, *J. Mol. Spectrosc.* **94**, 199–207 (1982).
34. F. Tamassia, S. M. Kermode, and J. M. Brown, *J. Mol. Spectrosc.* **205**, 92–101 (2001).
35. I. Lindgren and A. Rosén, *Case Stud. At. Phys.* 93–196, 197–298 (1974).
36. P. Pyykkö and M. Seth, *Theor. Chem. Acc.* **96**, 92–104 (1997).